ACS APPLIED MATERIALS & INTERFACES

www.acsami.org

Research Article

A Multienzyme Logic H^+ and Na^+ Biotransducer

Yukun Chen, Mingyin Cui, Bingfu Liu, Liyun Gao, Noriyo Mitome, Yoko Hirono-Hara, Kiyotaka Y. Hara, Gábor Méhes,* and Takeo Miyake*

Cite This: *ACS Appl. Mater. Interfaces* 2024, 16, 37521−37529

Read Online

ACCESS | Metrics & More | Article Recommendations | Supporting Information

ABSTRACT: Sodium ions and protons regulate various fundamental processes at the cell and tissue levels across all biological kingdoms. It is therefore pivotal for bioelectronic devices, such as biosensors and biotransducers, to control the transport of these ions through biological membranes. Our study explores the regulation of proton and sodium concentrations by integrating an Na^+-type ATP synthase, a glucose dehydrogenase (GDH), and a urease into a multienzyme logic system. This system is designed to operate using various chemical control input signals, while the output current corresponds to the local change in proton or sodium concentrations. Therein, a H^+ and Na^+ biotransducer was integrated to fulfill the roles of signal transducers for the monitoring and simultaneous control of Na^+ and H^+ levels, respectively. To increase the proton concentration at the output, we utilized GDH driven by the inputs of glucose and nicotinamide adenine dinucleotide (NAD^+), while recorded the signal change from the biotransducer, together acting as an AND enzyme logic gate. On the contrary, we introduced urease enzyme which hydrolyzed urea to control the decrease in proton concentration, serving as a NOT gate and reset. By integrating these two enzyme logic gates we formed a simple multienzyme logic system for the control of proton concentrations. Furthermore, we also demonstrate a more complex, Na^+-type ATP synthase-urease multienzyme logic system, controlled by the two different inputs of ADP and urea. By monitoring the voltage of the peak current as the output signal, this logic system acts as an AND enzyme logic gate. This study explores how multienzyme logic systems can modulate biologically important ion concentrations, opening the door toward advanced biological on-demand control of a variety of bioelectronic enzyme-based devices, such as biosensors and biotransducers.

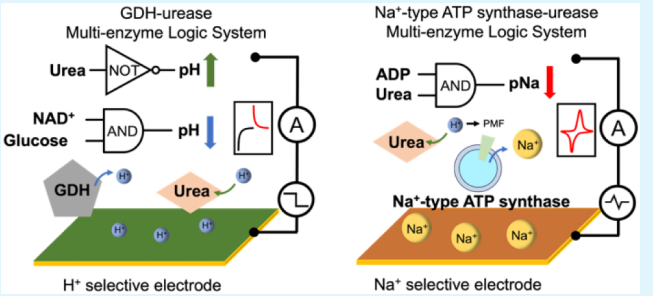

KEYWORDS: *ATP synthase, ion modulation, biotransducer, enzyme logic, multienzyme*

1. INTRODUCTION

In the field of bioelectronics, electronic systems are combined with biological processes to create innovative devices, such as biosensors for monitoring glucose,[1,2] lactate,[3] and ions.[4,5] Organic electronic conductors, including conducting polymers, are extensively used in merging biological and electrical systems, evident in innovations such as carbon nanotube-polydimethylsiloxane piezoelectric materials for pressure sensors,[6] conductive polymers for ion-selective electrodes,[7] electrochromic polymers combined with contact lenses,[8] organic electrochemical transistor sensing alcohol,[9] and controlled intracellular drug delivery by the doping properties of polymers.[10] Among them, solid-state and solution-based ion-selective electrodes have been widely used in biological research because of the importance of ions in fundamental biological processes, with examples of applications in calcium detection in biofluids,[11] proton transportation,[12] and potassium modulation[13] in supported lipid bilayers (SLBs)-ion channel systems. These works demonstrate the potential of ion-selective electrodes for bioelectronics and emphasize the importance of converting complex biological signals into electronic data. On the other hand, no work has been done in enzyme modulation by ion-selective electrodes to control sodium ions, even though these ions regulate various fundamental biological processes at the cellular and tissue levels, from photosynthetic and metabolic reactions[14] through the maintenance of electrolytic and fluid balance,[15] the transport of amino acids into cells,[16] to generating nerve impulses,[17] and beyond.

In biology, sodium and proton concentration gradients control ion transport systems during enzymatic activities, which fundamentally can be perceived as logical operations of biological signal modulation. Therefore, to enable the expression of ion signals in a more logical manner, enzyme logic systems[18,19] are a crucial research field in bioelectronics. This approach can take various forms, such as enzyme logic

Received: April 4, 2024
Revised: June 26, 2024
Accepted: July 1, 2024
Published: July 10, 2024

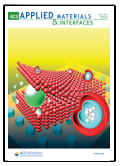

https://doi.org/10.1021/acsami.4c05499
ACS Appl. Mater. Interfaces 2024, 16, 37521−37529

network systems,[20] proton enzyme logic,[21−23] and multienzyme logic systems integrated into membranes,[24] to effectively bridge the gap between biological phenomena and electronic data processing. Even though several single-ion enzyme logic systems have been demonstrated, there is a need for integrated multi-ion control and complex multienzyme logic systems. These systems are essential for the modulation of complex biological processes, enabling more precise electronic signal processing in bioelectronic devices.

In this study, we designed a complex multienzyme logic system which we used to tune the ion concentrations of an electrolyte solution by applying appropriate combinations of biochemical input signals to this logic system, while we simultaneously monitored its activity as the electronic signal output of a biotransducer. More specifically, we integrated glucose dehydrogenase (GDH)-urease and Na^+-type ATP synthase-urease enzyme systems with Na^+ and H^+ biotransducer to simultaneously control and detect Na^+ and H^+ concentrations, respectively. This arrangement enhances our understanding of ion dynamics in biological contexts and highlights the potential of bioelectronics in creating interfaces between natural biochemical systems and electronic devices. The convergence of biology and electronics has the potential to revolutionize healthcare, diagnostics, and various biological applications.

2. EXPERIMENTAL SECTION

2.1. Materials. Poly(vinyl chloride) (high molecular weight; PVC), aniline (≥99.5% purity), magnesium chloride ($MgCl_2$), sodium ionophore X, 2-(*N*-morpholino)ethanesulfonic acid (MES), and fluorosulfonic acid (HSO_3F) were purchased from Sigma-Aldrich. GDH and urease were purchased from Toyobo Co. 3-*n*-Octylthiophene, *β*-D-glucose, bis(2-ethylhexyl) sebacate (or dioctyl sebacate, DOS), tetrabutylammonium hexafluorophosphate (NBu_4PF_6), sodium tetrakis[3,5-bis(trifluoromethyl)phenyl]borate (NaTFPB), and 1,2-dioleoyl-*sn*-glycero-3-phosphocholine (DOPC, >97.0% purity) were obtained from Tokyo Chemical Industry Co. Potassium dihydrogen phosphate (KH_2PO_4), lithium perchlorate ($LiClO_4$), potassium hydroxide (KOH), sucrose, urea, and tetrahydrofuran (super dehydrated, stabilizer free) were purchased from Wako Co. Acetonitrile (>99%), sodium chloride (NaCl), chloroform ($CHCl_3$), and potassium chloride (KCl) were purchased from Kishida Chemical Co. 3-Morpholinopropanesulfonic acid (MOPS), tricine, and HEPES were purchased from Dojindo Co. The substrates were 2-in. diameter silicon wafers purchased from Shunsheng Electronics Co. pH monitoring was done with a pH meter D-71 purchased from Horiba Scientific Co. The buffer solutions were prepared according to the recipe shown in Table S1, and the pH was adjusted with KOH. To modulate cation concentrations, K^+ concentrations were adjusted to 50 mM with KCl after adjustment of pH.

2.2. Fabrication of H^+ Biotransducer. In this study, the same method was used to fabricate sulfonated polyaniline (SPA) on gold electrodes as in our previous paper.[25] Briefly, H^+ biotransducer were fabricated on a silicon wafer with a SiO_2 insulating layer. First, a gold film was deposited by vacuum thermal evaporation, then aniline monomers were polymerized to yield SPA on the Au electrodes using cyclic voltammetry from −0.3 to 1.9 V in 100 mV/s scan rate for 15 cycles. Additionally, the H^+ biotransducer was combinate by coating a PDMS chamber on the gold electrode. The PDMS tank has dimensions of 2 cm × 2 cm × 0.8 cm (length x width x depth), and the selective electrode is positioned at the bottom surface of the PDMS tank, which also measures 2 cm × 2 cm.

2.3. Fabrication of Na^+ Biotransducer. The fabrication is based on the Au−POT−PVC three-layer structure preparation.[26,27] First, a poly(3-octylthiophene) (POT) layer was electrodeposited onto an Au electrode through the polymerization of 100 mM $LiClO_4$ and 100 mM 3-*n*-octylthiophene in acetonitrile, by an HSV-110 three-electrode potentiostat system (Hokuto Denko, Japan). Two cycles of cyclic voltammetry were applied, ranging from 0 V to +1.5 V (vs Ag/AgCl) at a sweep rate of 100 mV s^{-1} for electrodeposition. Then, 0 V was applied for 120 s to stabilize the oxidation state of POT, followed by a 30 min immersion in pure acetonitrile to remove the surface electrolyte and a 30 min air-drying at room temperature. In the case of the PVC layer, a PVC−THF cocktail solution was prepared using 6.6 mg of PVC, 12.6 mg of DOS, 1.7 mg of NaTFPB, and 0.7 mg of sodium ionophore X in 1 mL of THF. To create the PVC layer, 50 μL of the diluted PVC−THF solution (cocktail solution: THF = 1:4) was drop-coated, and then spin-coated at 1500 rpm for 120 s, followed by drying at room temperature for 15 min. The same PDMS chamber was used in Na^+ biotransduer.

2.4. ATP Synthase Preparation. In this study, we utilized the plasmid pTR-hF$_1$F$_{o(-i)}$[28] for the expression of Na^+-type ATP (F_o from *P. modestum*, and F_1 from *Bacillus* PS3) with a 10-histidine tag at the N-terminus of each *β*-subunit. Na^+-type ATP synthase was expressed in an F_oF_1 ATP synthase-deficient *E. coli* strain JM103 Δ(*uncB-uncD*) with plasmid pTR-hF$_1$F$_{o\ (-i)}$ and plasmid PST-I.[28] The culture of the transformants, the preparation of the membrane vesicles, and the purification of the Na^+-type ATP synthase were performed as described.[25] Protein concentrations were determined by using the BCA protein assay kit (Takada), with bovine serum albumin serving as a standard.

2.5. Liposome Preparation, Restitution, and Acidification. DOPC powder was dissolved in chloroform, evaporated by N_2 gas, and redissolved in vesicle buffer solution (the compositions of all buffer solutions are listed in Table S1) to yield 40 mg mL^{-1} DOPC solution. The prepared DOPC solution was ultrasonicated for 10 min, and the vesicles were collected using a 100 nm diameter filter 10 times. The enzyme restitution solution was prepared by adding 75 μg of Na^+-type ATP synthase into 250 μL DOPC solution and 750 μL vesicle buffer solution, and incubated at 25 °C for 2 h. For acidification, 300 μL of incubated restitution solution was mixed with 700 μL of acidification buffer solution, and incubated at 23−27 °C for 10−20 h to obtain the incubated solution.

2.6. ATP Concentration Measurement. We used the same ATP assay kit (Roche, ATP Bioluminescence Assay Kit CLS II) and microplate reader (Fluoroskan FL, Thermo Scientific) as described previously. All the preparation and detection procedures were as described previously.[25]

2.7. Electrical Measurements. For the open-circuit voltage (OCV) measurement, the H^+ transducer and Ag/AgCl (3 M KCl) electrode served as the working and reference electrodes, respectively, as two-electrode system. For the current measurement of SPA threshold and GDH-urease enzyme logic, the SPA working electrode, Pt wire counter electrode, and Ag/AgCl reference electrode were connected to a three-electrode potentiostat, applied 0.0 V for 5 s for initialization, charged voltage for 30 s, and discharged voltage for 30 s in 0.5 M Na_2SO_4 solution. In the GDH condition, proton current which shows proton releasing and absorbing reaction on electrode was measured in 0.5 M Na_2SO_4 (pH 6.7) containing 1 mg GDH in the presence and absence of 30 mM glucose and 1 mM nicotinamide adenine dinucleotide (NAD^+). In the urease condition, proton current was measured in 0.5 M Na_2SO_4 (pH 5.6) in the presence and absence of 5 units mL^{-1} urease and 4 mM urea, respectively. For the cyclic voltammetry (CV) measurements, the Na^+ biotransducer, Pt wire, and Ag/AgCl (KCl) electrodes were connected as the working, counter, and reference electrodes, respectively. Cyclic voltammograms ranging from 0 V to +0.8 V (vs Ag/AgCl) were applied for 10 cycles at a sweep rate of 100 mV s^{-1}. For sodium selectivity measurement, the experiment was performed under different NaCl concentrations and different pH reaction buffer solutions. For ATP synthase reaction, the solution, mixed with 400 μL of incubated solution and 1600 μL of reaction buffer solution, was measured in the presence and absence of 2 mM ADP. For ATP synthase enzyme logic measurement, the solution mixed with 400 μL of incubated solution and 1600 μL of reaction buffer solution in the presence and absence of 2 mM ADP and 4 mM urease, respectively, was measured. All the measurements were done by using an HSV-110 (Hokuto Denko, Japan).

https://doi.org/10.1021/acsami.4c05499
ACS Appl. Mater. Interfaces 2024, 16, 37521−37529

3. RESULTS AND DISCUSSION

3.1. Description of the Multienzyme Logic System. To prepare a multi-ion controlled multienzyme logic system, different ion biotransducers need to be integrated with different ion-controllable enzyme logic systems. To realize such a complex system, we first prepared an H^+ biotransducer by electrochemically depositing an SPA layer on top of a gold film. Simultaneously, we created a Na^+ biotransducer by combining an electrochemically deposited POT layer with a spin-coated PVC film. These two biotransducers were incorporated into an enzyme logic system composed of GDH-urease and Na^+-type ATP synthase-urease, specifically devised for modulating H^+ and Na^+ concentrations, respectively, in a buffer solution containing a mixture of incubated and reaction buffer solutions, placed within a PDMS chamber, as shown in Figure 1. In the GDH-urease enzyme logic system, NAD^+ and glucose work as two inputs of an AND gate, modulating the increase in proton concentration, while urea works as a NOT gate input and reset, modulating the decrease in proton concentration. On the other hand, in the Na^+-type ATP synthase-urease enzyme logic system, ADP and urea act as two inputs of an AND gate, modulating the increase in Na^+ concentration. The integration of multi-ion biotransducer with multienzyme logic systems holds the promise of an important tool for realizing advanced bioelectronic devices capable of complex biological interactive functions.

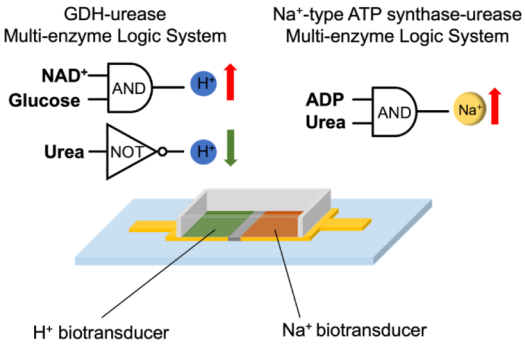

Figure 1. Principle of proton-controlled and sodium-controlled multienzyme logic systems device. The AND and NOT logic enzyme systems integrate a H^+ biotransducer with the GDH-urease multienzyme to regulate the proton signal with inputs of glucose, NAD^+, and urea. Another AND logic enzyme system integrates an Au−POT−PVC electrode with the Na^+-type ATP synthase-urease multienzyme system to regulate the sodium signal with inputs of urea and ADP.

3.2. Validation of Electrochemical Performance of H^+ Biotransducer. To detect changes in proton concentrations in the enzyme logic system, we employed SPA,[29] a proton-selective conductive polymer that functions as a biotransducer from ionic to electrical signal.[30,31] Specifically, we monitored the OCV between the SPA electrode and a Ag/AgCl reference electrode in buffer solutions with pH values of 5.6, 6.6, 7.7, and 8.4. To verify that the SPA electrode is not affected by changes in sodium levels, we evaluated its selectivity for protons for three different sodium concentrations, starting the recording with 0.1 mM NaCl, then adjusting the NaCl concentration to 0.5 mM at 80 s and to 1 mM NaCl at 120 s (Figure 2a). The OCV value increased with increasing proton concentration at 50 mV/decade change, which correlates to the Nernst equation as a result of the proton selectivity of the SPA electrode. Furthermore, the OCV value remained stable when the sodium concentration increased, indicating that the SPA is not affected by changes in the sodium level.

Next, to confirm that proton concentrations in the solution are proportional to the polarization state of SPA, our study continued with charge and discharge reactions under specific potential conditions. This was achieved by applying a reduction threshold voltage (Vr) to SPA, leading to its reduction by absorbing protons from the solution and transitioning the SPA into a reduced state. The key evidence for this reduction process is the doping proton current observed when the potential is subsequently set to 0 V (all voltage values are given in reference to Ag/AgCl). This current indicates the flow of protons released by the protonated SPA into the solution, a process that can be influenced by the pH level of the buffer solution. For example, when pH = 5, the Vr is determined to be +0.24 V, as shown in Figure S1. Under

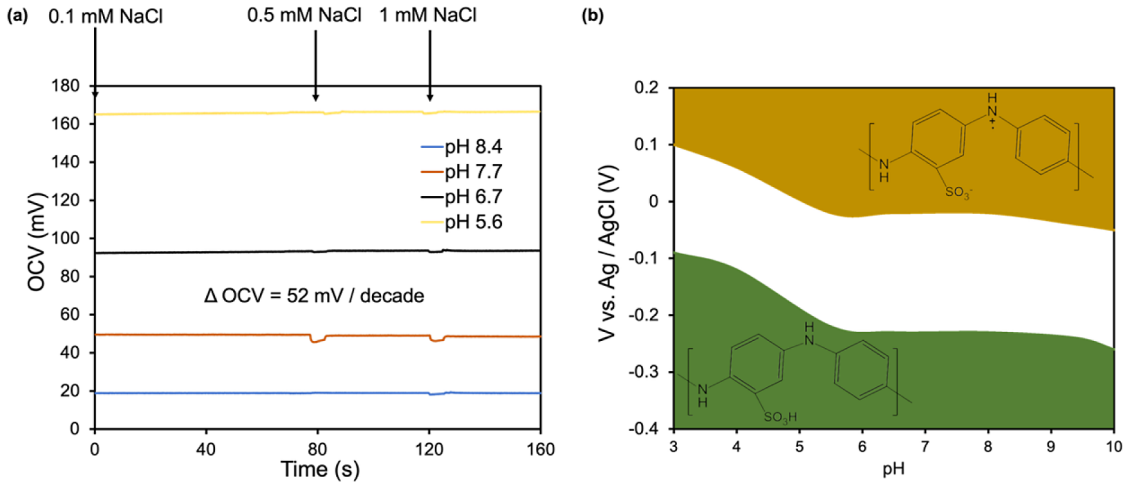

Figure 2. Evaluation of electrochemical performance of SPA H^+ biotransducer. (a) Temporal evolution of OCV of SPA in buffer solutions with pH 5.6, 6.7, 7.7, and 8.4, where the NaCl concentration of the solution is 0.1 mM, 0.5 mM, and 1 mM at t = 0, 80, and 120 s, respectively. (b) Map of SPA threshold voltages Vr and Vo in buffer solutions with different pH. Green and yellow areas represent the reduction and oxidation states of SPA, respectively. Inset images in (b) show the molecular structures of SPA at the corresponding reduced and oxidized states.

https://doi.org/10.1021/acsami.4c05499
ACS Appl. Mater. Interfaces 2024, 16, 37521−37529

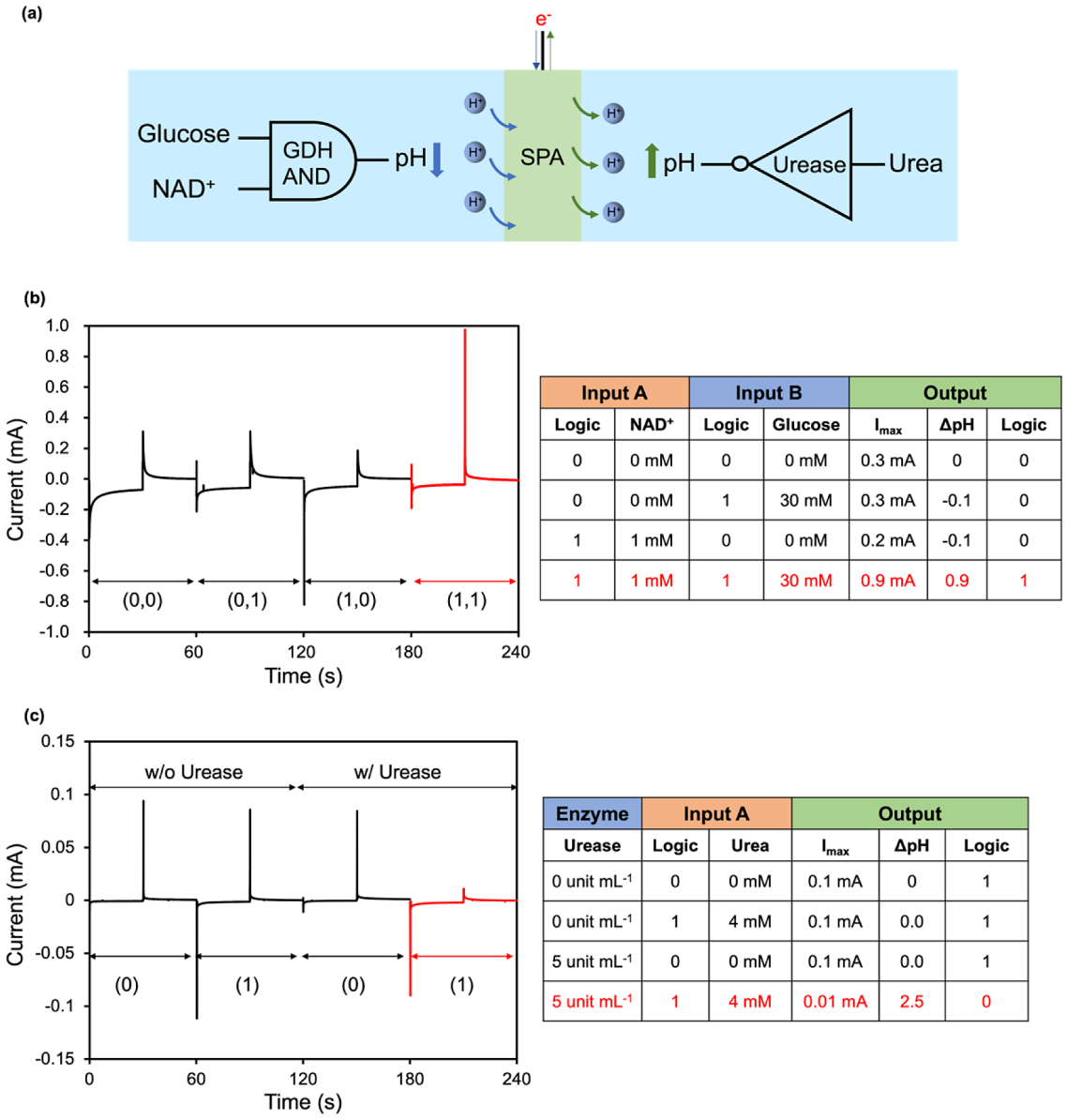

Input A		Input B		Output		
Logic	NAD^+	Logic	Glucose	I_{max}	ΔpH	Logic
0	0 mM	0	0 mM	0.3 mA	0	0
0	0 mM	1	30 mM	0.3 mA	-0.1	0
1	1 mM	0	0 mM	0.2 mA	-0.1	0
1	1 mM	1	30 mM	0.9 mA	0.9	1

Enzyme	Input A		Output		
Urease	Logic	Urea	I_{max}	ΔpH	Logic
0 unit mL^{-1}	0	0 mM	0.1 mA	0	1
0 unit mL^{-1}	1	4 mM	0.1 mA	0.0	1
5 unit mL^{-1}	0	0 mM	0.1 mA	0.0	1
5 unit mL^{-1}	1	4 mM	0.01 mA	2.5	0

Figure 3. Proton concentrations in buffer solution controlled by GDH and urease enzyme logic systems via an SPA H^+ biotransducer. (a) Schematic of detection of proton signal changes by SPA electrode induced by GDH-urease multienzyme system. GDH performs AND logic with NAD^+ and glucose as inputs, decreasing the pH in solution and producing proton current as output. Urease performs NOT logic with urea as input, increasing the pH in solution and proton current as output. (b) GDH enzyme logic regulates the proton current of the SPA electrode in different input conditions and its corresponding AND gate truth table. (c) Urease enzyme logic regulates the proton current of the SPA electrode in different input conditions and its corresponding NOT gate truth table. The red lines and arrows in the graphs and red letters in the truth table in (b) and (c) represent the conditions when input and output are (1,1) and 1 (for (b)), and 1 and 0 (for (c)), respectively.

these conditions, when the potential is at or below Vr and is then adjusted to 0 V, the doping proton current is distinctly observed, confirming the proton-driven reduction process in SPA. Conversely, applying an oxidation threshold voltage (Vo) after first applying Vr sets the proton doping current close to zero. This negligible current indicates that there is no flow of protons from the oxidized SPA film into the solution, a process that again can vary with the pH level of the buffer solution. As shown in Figure S2, when pH = 6.5, Vo is −0.15 V, confirming the oxidation state of SPA by the absence of a doping proton current after Vo is applied.

The voltage threshold map for the SPA electrode is presented in Figure 2b, summarizing the measurements taken at every 0.5 pH unit from pH 3 to pH 10. From this map, we can clearly see that from pH 3 to pH 6, a linear correlation exists between the threshold voltage change and the pH change. Therefore, the variation of Vr with pH allows us to use the SPA electrode to track proton concentration changes in the form of electrical signal readout, suggesting a potential for enzymatic logic systems.

3.3. Preparation and Evaluation of SPA Electrode-Based Proton Logic System. To detect the proton concentration variations caused by enzyme reactions, we integrated the H^+ biotransducer into the GDH logic system. We utilized SPA as a proton sensor and demonstrated the detection of pH decrease via an AND logic gate, where GDH was controlled by NAD^+ and glucose, two chemical inputs. In addition, we introduced a NOT logic gate based on a urease

https://doi.org/10.1021/acsami.4c05499
ACS Appl. Mater. Interfaces 2024, 16, 37521−37529

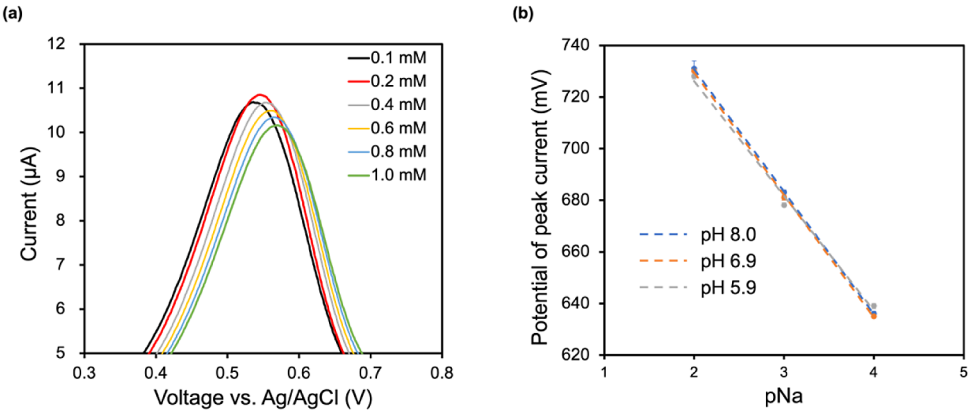

Figure 4. Evaluation of Au−POT−PVC Na^+ biotransducer performance. (a) CVs recorded with the Na^+ biotransducer at a 100 mV s^{-1} scan rate in a pH 6.7 buffer solution, at NaCl concentrations of 0.1 mM, 0.2 mM, 0.4 mM, 0.6 mM, 0.8 mM, and 1.0 mM. (b) Calibration curves (dashed lines) based on peak current potentials (symbols) obtained from CVs at different Na^+ concentrations (pNa) in pH 5.9, 6.9, and 8.0 buffer solutions.

enzyme that increases pH, controlled by the input of urea, the latter corresponding to a reset signal (Figure 3a).

To confirm the logic working principle of GDH enzyme, we measured the SPA proton current as output in the presence and absence of NAD^+ and glucose as two different inputs by applying the same Vr for 30 s and 0 V for 30 s. The duration of 30 s was selected because, after approximately 15 s, the current becomes relatively gentle, and the SPA reaction reaches saturation. The current, pH, and output current values in the truth table under four input conditions: (0,0), (0,1), (1,0), and (1,1), along with the assignment of logical values to physical parameters, are summarized in Figure 3b. The maximum proton current was observed in the solution containing 1 mM NAD^+ and 30 mM glucose, corresponding to inputs (1,1). This can be attributed to the increase of protons in the solution through the reactions of NAD^+ and glucose, resulting in a change in the pH of the solution, in turn altering the threshold voltage. The proton current exhibited low values under (0,0), (0,1), and (1,0) input logic conditions due to the unchanging pH of the solution. The pH value significantly decreased only in logic condition (1,1), and the resulting high output current condition, measured on the SPA electrode, was regarded as logic output = 1. Thus, we managed to integrate our H^+ biotransducer with an AND logic gate in which the output signal was activated by two chemical inputs: glucose and NAD^+. These inputs are effectively regulated by the proton doping reaction in SPA electrode, which is ultimately driven by the GDH enzyme.

Next, to confirm the working principle of the urease enzyme logic system, we measured the SPA proton current as output by first applying the same Vr for 30 s and then 0 V for 30 s in the presence and absence of urease and urea as the input and enzyme logic, respectively. The proton current and pH values for different cases in the truth table are summarized in Figure 3c. We found that the minimum proton current corresponds to the solution containing both urea (4 mM) and urease (5 units/mL). The reason behind this is the hydrolysis of NH_3 from urea by urease which then reacted with water and generated OH^- to increase the pH, in turn changing the threshold voltage. This cascade resulted in an increased pH and decreased current, effectively integrating a proton-controlled NOT logic and a reset function, where reset means the pH returns to its original level. When urea is added and the output is returned to 0, the pH reset facilitates enzyme-based logic to return to the original pH, allowing for effective detection of repetitions.

Together, by integrating H^+ biotransducer with GDH and urease enzymes, we successfully developed a simple multienzyme logic system that can control proton concentrations, and is capable of executing AND and NOT logic operations through the detection of pH variations, demonstrating a versatile approach for biochemical sensing and signal processing. The circuit diagram and reaction mechanism are shown in Figure S3.

3.4. Na^+ Biotransducer Fabrication and Performance.

So far, we have only discussed proton ion environment; to detect multiple ions and convert them into electrical signals, we chose a solid-state Na^+ biotransducer for the monitoring of Na^+ concentrations in a multienzyme logic system. The Na^+ biotransducer, fabricated on a gold substrate[32] and mechanism were as shown in Figure S4, consists of poly(3-octylthiophene) (POT) as an ion-to-electron transducer layer, and a PVC film as a sodium-selective membrane.[33] By comparing CV measurements in a 0.1 M NBu_4PF_6 solution at different scan rates, we found a linear correlation between the maximum current density values and the applied voltage, pointing to a strong reversible oxidation reaction of POT[34] (Figure S5). According to the working mechanism of the Na^+ biotransducer, when a voltage is applied to the gold-coated glass substrate, electron transfer occurs between the ion-to-electron transducer layer and the gold conducting layer, resulting in a shift from the oxidized state (POT^+) to the neutral state (POT). For sodium selectivity, a PVC membrane containing sodium ionophore X and the cation exchanger TFPB is deposited on the POT layer. TFPB performs ion exchange between the POT layer,[35] and the ionophore can capture and release sodium ions, resulting in the PVC layer exhibiting sodium selectivity.

To evaluate the selectivity of the Na^+ biotransducer, we used CV to determine the current peaks in sodium solutions with different concentrations (Figure 4a; the full CVs are shown in Figure S6). Oxidation and reduction peak currents were observed at approximately 0.5 V, indicating the release and absorption of sodium, respectively. A gap of approximately 0.1 V between the oxidation and reduction peaks is caused, we believe, by interfacial defects between the PVC and POT layers.[36] The voltage of the peak current increases linearly with increasing sodium concentrations in buffer solutions in the

https://doi.org/10.1021/acsami.4c05499
ACS Appl. Mater. Interfaces 2024, 16, 37521−37529

order of 0.1 mM, 0.2 mM, 0.4 mM, 0.6 mM, 0.8 mM, 1 mM, and 10 mM. The voltage change is approximately 40 mV/decade for each 10-fold increase in concentration, indicating relatively good sodium selectivity based on the Nernst equation (Figure 4). Simultaneously, we observed an excellent sodium selectivity for each 10-fold increase in concentrations from 100 μM to 100 mM NaCl (Figure S5). These results demonstrate that the Au−POT−PVC electrode can function as a Na^+ sensor with 0.1 mM detection accuracy and a wide range of detection.

Next, to confirm that protons have no effect on sodium selectivity in the Na^+ biotransducer, we determined the potential values at the peak currents from CV measurements in buffer solutions with different proton and sodium concentrations. The relationship between the potential and the negative decimal logarithm of Na^+ ion concentration (pNa) is shown in Figure 4b. We observed that a 10-fold change in Na^+ ion concentration leads to a change of 47.5 mV, 47 mV, and 45.5 mV at pH 8.0, 6.9, and 5.9, respectively. This result shows that the proton concentration does not significantly affect the detection of sodium by the Na^+ biotransducer. Finally, we note that the fabrication process of the Na^+ biotransducer could not be consistently controlled to have negligible variations between individual electrodes due to the difficulty in precisely controlling the POT thickness and its surface morphology. As a result, this caused variations in the thickness of the PVC layer, leading to device-to-device differences in potentials at which the peak currents evolved.

3.5. Na^+-Type ATP Synthase Reaction in Vesicle. The ATP synthesis reaction of ATP synthase occurs with ions transported through the vesicle, powered by ADP molecules and the ionic gradient across vesicles.[37] In the case of Na^+-type ATP synthase, Na^+ can be transported across the vesicle driven by the force of proton gradient, called the proton motive force (PMF).[28] To confirm that ATP synthesis is driven by ADP and PMF, we measured the concentration of ATP synthesized by the Na^+-type ATP synthase. To generate different PMF values, we created different pH gradients (ΔpH) across the vesicles, then measured the ATP concentration in the presence and absence of ADP. Because the sodium concentration is equal between vesicles, the force of the entire ionic medium is determined solely by the concentration of protons. Figure 5a displays the changes in ATP concentrations measured 3 min after adding ADP molecules at various ΔpH conditions across the vesicles. The ΔpH can be calculated from the Nernst equation. When ΔpH was raised to 2.4 (PMF = 140 mV) and ADP was present, the concentration of ATP increased significantly compared to the control experiment at the same ΔpH but without ADP. On the other hand, ATP concentrations measured at values of ΔpH lower than 2.4 did not differ from the control even in the presence of ADP, as shown in Figure 4a for ΔpH = 1.6 (PMF = 95 mV) and 0.8 (PMF = 47 mV). These results confirm that when PMF was set to 140 mV, the presence of ADP molecules can trigger ATP synthesis in Na^+-type ATP synthase.

To confirm the transport of sodium ions through ATP synthase during ATP synthesis, we plot the potential values at peak currents in the presence and absence of ADP and 140 mV of PMF (ΔpH = 2.4), respectively, using our Na^+ biotransducer (Figure 5b). The results clearly demonstrated a higher peak current potential in the presence of both ADP and 140 mV of PMF, compared to other combinations,

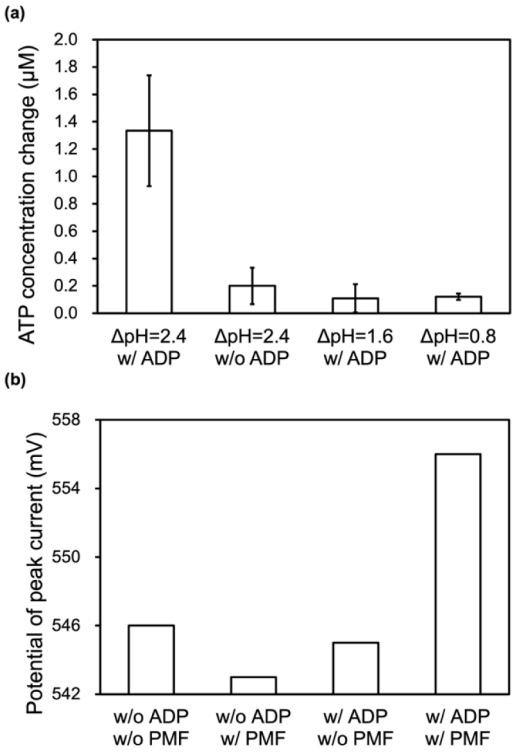

Figure 5. Performance of ATP synthesis reaction of Na^+-type ATP synthase driven by ADP and proton motive force (PMF) created by proton gradients (ΔpH). (a) ATP concentration changes were measured in the presence and absence of ADP at varying ΔpH values. (b) Sodium concentration changes were detected through potential of peak current obtained from cyclic voltammetry (CV) in the presence and absence of PMF and ADP molecules.

confirming that sodium ions were transported through the vesicle driven by ADP and PMF.

3.6. Na^+-Type ATP Synthase Combined with Urease Enzyme Logic System. As discussed above, we observed that urease functions as a NOT logic gate, triggering an increase in the solution's pH in response to the presence of urea. This finding provides the basis for combining urease with Na^+-type ATP synthase for creating a Na^+ controlled-enzyme logic system. Through the hydrolysis of urea, urease releases protons into the solution, creating a proton gradient across the vesicle that acts as PMF. This complex multienzyme logic system, using ADP and urea as inputs, regulates Na^+ transport across vesicles within the ATP synthesis reaction. The output signal, which corresponds to the concentration change of Na^+ in the solution, is detected as a potential signal by a Na^+ biotransducer.

In our model, ADP is designated as input A and urea as input B (Figure 6a). To confirm the operation of the enzyme logic, we observed the potential of the peak currents during CV scans ranging from 0 to +0.8 V in both the presence and absence of urea and ADP under four distinct input scenarios, (0,0), (0,1), (1,0), and (1,1), shown in Figure 6a. The values are summarized in a truth table (Figure 6b). Our observations revealed that the potential attained its maximum value in a solution containing 4 mM urea and 10 mM ADP. This effect is attributed to the hydrolysis of urea by urease, which results in the generation of OH^- in the solution and PMF across the vesicle membrane (Figure S7). The presence of ADP and the generated PMF facilitate the ATP synthesis in ATP synthase;

https://doi.org/10.1021/acsami.4c05499
ACS Appl. Mater. Interfaces 2024, 16, 37521−37529

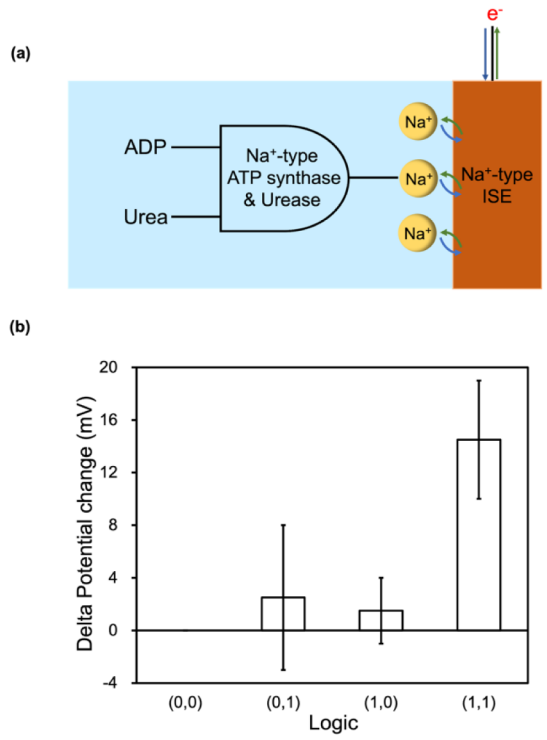

Input A ADP		Input B Urea		Output Peak Current potential /$c_{(Na+)}$	
Logic	ADP	Logic	Urea	Logic	Potential change(mV)
0	0 mM	0	0 mM	0	0
0	2 mM	0	0 mM	0	2.5
1	0 mM	1	4 mM	0	1.5
1	2 mM	1	4 mM	1	14.5

Figure 6. Sodium concentrations controlled in buffer solution by enzyme logic system. (a) Schematic of the Na^+ biotransducer, detecting sodium signal generated by Na^+-type ATP synthase-urease multienzyme system acting as an AND logic, where urea and ADP are inputs and sodium current is output. (b) Enzyme logic regulates variations of potential in the Na^+ biotransducer under different input conditions and its corresponding AND gate truth table.

meanwhile, sodium ions are transported from the vesicle into the solution. This ion transport induces a large change of 14.6 mV in the potential of the Na^+ biotransducer, which is interpreted as output = 1 in our system (Figure 6b). Under the (0,0), (0,1), and (1,0) conditions, only minimal variations in the potential of the peak currents were observed, indicating that sodium was not transported from the vesicle into the solution, and thus, these conditions are classified as output = 0. In conclusion, we managed to integrate our Na^+ biotransducer with an AND logic gate in which the output signal was activated by two chemical inputs: urea and ADP. These inputs can effectively regulate the Na^+-type ATP synthase-urease multienzyme logic system.

4. CONCLUSIONS

In this research, we have developed a complex multienzyme logic system that regulates proton and sodium ion concentrations by controlling enzyme reactions through chemical inputs. We used the combination of H^+ and Na^+ biotransducers to convert concentration variation inputs into electrical signal outputs. We first demonstrated the functionality of the H^+ biotransducer through OCV measurements and threshold voltage mapping. This biotransducer was integrated into the GDH enzyme logic system, acting as an AND gate to provide output variations in H^+ concentrations in response to glucose and NAD^+ inputs. Also, we introduced urease into solution, which uses urea as an input and acts as a NOT gate and a system reset, thereby creating a simple proton-controlled multienzyme logic system. To explore multi-ion environments, we demonstrated the operation of a highly selective Na^+ biotransducer by CV measurements in the presence of different pH buffer solutions with varying Na^+ concentrations. We introduced the Na^+-type ATP synthase into lipid vesicle solution and confirmed that ATP synthesis is followed by sodium ion transport driven by ADP and PMF. Subsequently, to establish a Na^+-controlled multienzyme logic system, we combined the Na^+-type ATP synthase with urease. Therein, urease regulates the proton concentration in the solution, generating PMF across the vesicle. Furthermore, we created a complex enzyme logic gate where ADP and urea were two inputs, controlling Na^+ transport in Na^+-type ATP synthase, and where variations in sodium-ion concentrations were converted into electrical signals by the Na^+ biotransducer, serving as the output. The multienzyme logic systems hold significant potential for diverse applications in medical diagnostics, drug development, and biological research. It can detect disease biomarkers for early diagnosis and personalized treatment, perform high-throughput screening and real-time monitoring in drug development, and control and monitor complex biological processes. Additionally, it serves as a foundational component for advanced bioelectronic and iontronic microdevices, regulating and sensing ion concentrations in both biological and artificial systems. This has further applications in medicine, bioengineering, and beyond.

■ ASSOCIATED CONTENT

Supporting Information

The Supporting Information is available free of charge at https://pubs.acs.org/doi/10.1021/acsami.4c05499.

SPA reduction threshold voltage measurement; SPA oxidation threshold voltage measuremnet; structure and mechanism of Na^+ biotransducer; cyclic voltammetry curves of Au−POT; evaluation of Au−POT−PVC Na^+ biotransducer; principle of the Na^+-type ATP synthase-urease enzyme logic system; and compositions of buffer solutions (PDF)

■ AUTHOR INFORMATION

Corresponding Authors

Gábor Méhes − *Graduate School of Information, Production and Systems, Waseda University, Kitakyushu, Fukuoka 808-0135, Japan;* orcid.org/0000-0003-4859-1359; Email: mehes.gabor@aoni.waseda.jp

Takeo Miyake − *Graduate School of Information, Production and Systems, Waseda University, Kitakyushu, Fukuoka 808-0135, Japan; PRESTO, Japan Science and Technology Agency, Saitama 332-0012, Japan;* orcid.org/0000-0002-7445-633X; Email: miyake@waseda.jp

Authors

Yukun Chen − *Graduate School of Information, Production and Systems, Waseda University, Kitakyushu, Fukuoka 808-0135, Japan*

Mingyin Cui − *Graduate School of Information, Production and Systems, Waseda University, Kitakyushu, Fukuoka 808-0135, Japan*
Bingfu Liu − *Graduate School of Information, Production and Systems, Waseda University, Kitakyushu, Fukuoka 808-0135, Japan*
Liyun Gao − *Graduate School of Information, Production and Systems, Waseda University, Kitakyushu, Fukuoka 808-0135, Japan*
Noriyo Mitome − *Faculty of Education, Tokoha University, Shizuoka, Shizuoka 422-8581, Japan*
Yoko Hirono-Hara − *Department of Environmental and Life Sciences, School of Food and Nutritional Sciences, University of Shizuoka, Shizuoka, Suruga-ku 422-8526, Japan*
Kiyotaka Y. Hara − *Department of Environmental and Life Sciences, School of Food and Nutritional Sciences, University of Shizuoka, Shizuoka, Suruga-ku 422-8526, Japan*

Complete contact information is available at: https://pubs.acs.org/10.1021/acsami.4c05499

Author Contributions

T.M. conceived the study. T.M., Y.C., and N.M. designed the experiments. Y.C., B.L., L.G., M.C., and N.M. performed the experiments. Y.C., M.C., and T.M. analyzed the data. N.M., Y.H.H., and K.Y.H. prepared the ATP synthase. Y.C., G. M., M.C., and T.M. wrote the manuscript.

Notes

The authors declare no competing financial interest.

■ ACKNOWLEDGMENTS

This study was supported by JST and PRESTO (Grant Number: JPMJPR20B8). A portion of this work was conducted at the Kitakyushu Foundation for the Advancement of Industry, Science, and Technology, Semiconductor Center, and supported by the Nanotechnology Platform Program of the Ministry of Education, Culture, Sports, Science, and Technology, Japan. Noriyo Mitome was supported by the Cooperative Research Program of the NJRC Mater. & Dev. We thank Dr. Toshiharu Suzuki and Dr. Masasuke Yoshida for providing the expression plasmid for ATP synthase.

■ REFERENCES

(1) Yin, S.; Yu, Z.; Song, N.; Guo, Z.; Li, W.; Ma, J.; Wang, X.; Liu, J.; Liang, M. A Long Lifetime and Highly Sensitive Wearable Microneedle Sensor for the Continuous Real-Time Monitoring of Glucose in Interstitial Fluid. *Biosens. Bioelectron.* **2024**, *244*, 115822.
(2) Diacci, C.; Lee, J. W.; Janson, P.; Dufil, G.; Méhes, G.; Berggren, M.; Simon, D. T.; Stavrinidou, E. Real-Time Monitoring of Glucose Export from Isolated Chloroplasts Using an Organic Electrochemical Transistor. *Adv. Mater. Technol.* **2020**, *5* (3), 1900262.
(3) Méhes, G.; Roy, A.; Strakosas, X.; Berggren, M.; Stavrinidou, E.; Simon, D. T. Organic Microbial Electrochemical Transistor Monitoring Extracellular Electron Transfer. *Adv. Sci.* **2020**, *7* (15), 2000641.
(4) Keene, S. T.; Fogarty, D.; Cooke, R.; Casadevall, C. D.; Salleo, A.; Parlak, O. Wearable Organic Electrochemical Transistor Patch for Multiplexed Sensing of Calcium and Ammonium Ions from Human Perspiration. *Adv. Healthcare Mater.* **2019**, *8* (24), 1901321.
(5) Nyein, H. Y. Y.; Gao, W.; Shahpar, Z.; Emaminejad, S.; Challa, S.; Chen, K.; Fahad, H. M.; Tai, L.-C.; Ota, H.; Davis, R. W.; et al. A Wearable Electrochemical Platform for Noninvasive Simultaneous Monitoring of Ca2+ and pH. *ACS Nano* **2016**, *10* (7), 7216−7224.
(6) Azhari, S.; Kimizuka, K.; Méhes, G.; Usami, Y.; Hayashi, Y.; Tanaka, H.; Miyake, T. Integration of Wireless Power Transfer Technology With Hierarchical Multiwalled Carbon Nanotubes-Polydimethylsiloxane Piezo-Responsive Pressure Sensor for Remote Force Measurement. *IEEE Sens. J.* **2023**, *23* (7), 7902−7909.
(7) Crespo, G. A.; Cuartero, M.; Bakker, E. Thin Layer Ionophore-Based Membrane for Multianalyte Ion Activity Detection. *Anal. Chem.* **2015**, *87* (15), 7729−7737.
(8) Hu, L.; Chen, L.; Du, N.; Takamatsu, T.; Xiao, T.; Miyake, T. Electrochromic Soft Contact Lenses with Built-in Non-Interfering, High-Efficient Dual-Band Wireless Power Transfer System. *Sens. Actuators, A* **2022**, *344*, 113766.
(9) Bihar, E.; Deng, Y.; Miyake, T.; Saadaoui, M.; Malliaras, G. G.; Rolandi, M. A Disposable Paper Breathalyzer with an Alcohol Sensing Organic Electrochemical Transistor. *Sci. Rep.* **2016**, *6* (1), 27582.
(10) Zhang, B.; Zheng, D.; Yiming, S.; Oyama, K.; Ito, M.; Ikari, M.; Kigawa, T.; Mikawa, T.; Miyake, T. High-Efficient and Dosage-Controllable Intracellular Cargo Delivery through Electrochemical Metal−Organic Hybrid Nanogates. *Small Sci.* **2021**, *1* (12), 2100069.
(11) Xu, G.; Cheng, C.; Yuan, W.; Liu, Z.; Zhu, L.; Li, X.; Lu, Y.; Chen, Z.; Liu, J.; Cui, Z.; et al. Smartphone-Based Battery-Free and Flexible Electrochemical Patch for Calcium and Chloride Ions Detections in Biofluids. *Sens. Actuators, B* **2019**, *297*, 126743.
(12) Hemmatian, Z.; Keene, S.; Josberger, E.; Miyake, T.; Arboleda, C.; Soto-Rodríguez, J.; Baneyx, F.; Rolandi, M. Electronic Control of H+ Current in a Bioprotonic Device with Gramicidin A and Alamethicin. *Nat. Commun.* **2016**, *7* (1), 12981.
(13) Imai, K.; Horio, T.; Hattori, T.; Sawada, K.; Tero, R. Lipid Bilayer Formation on an Ion Image Sensor and Measurement of Time Response of Potential Dependency on Ion Concentration. *Jpn. J. Appl. Phys.* **2019**, *58* (SD), SDDK06.
(14) Kimmich, G. A. Active Sugar Accumulation by Isolated Intestinal Epithelial Cells. A New Model for Sodium-Dependent Metabolite Transport. *Biochemistry* **1970**, *9* (19), 3669−3677.
(15) Hyndman, K. A.; Speed, J. S.; Mendoza, L. D.; Allan, J. M.; Colson, J.; Sedaka, R.; Jin, C.; Jung, H. J.; El-Dahr, S.; Pollock, D. M.; Pollock, J. S. Fluid-Electrolyte Homeostasis Requires Histone Deacetylase Function. *JCI Insight* **2020**, *5* (16), No. e137792.
(16) Bussolati, O.; Dall'asta, V.; Franchi-Gazzola, R.; Sala, R.; Rotoli, B. M.; Visigalli, R.; Casado, J.; Lopez-Fontanals, M.; Pastor-Anglada, M. A.; Gazzola, G. C. The Role of System A for Neutral Amino Acid Transport in the Regulation of Cell Volume. *Mol. Membr. Biol.* **2001**, *18* (1), 27−38.
(17) Devor, M. Sodium Channels and Mechanisms of Neuropathic Pain. *J. Pain* **2006**, *7* (1, Supplement), S3−S12.
(18) Katz, E.; Privman, V. Enzyme -Based Logic Systems for Information Processing. *Chem. Soc. Rev.* **2010**, *39* (5), 1835−1857.
(19) Hemmatian, Z.; Miyake, T.; Deng, Y.; Josberger, E. E.; Keene, S.; Kautz, R.; Zhong, C.; Jin, J.; Rolandi, M. Taking Electrons out of Bioelectronics: Bioprotonic Memories, Transistors, and Enzyme Logic. *J. Mater. Chem. C* **2015**, *3* (25), 6407−6412.
(20) Privman, M.; Tam, T. K.; Pita, M.; Katz, E. Switchable Electrode Controlled by Enzyme Logic Network System: Approaching Physiologically Regulated Bioelectronics. *J. Am. Chem. Soc.* **2009**, *131* (3), 1314−1321.
(21) Miyake, T.; Josberger, E. E.; Keene, S.; Deng, Y.; Rolandi, M. An Enzyme Logic Bioprotonic Transducer. *APL Mater.* **2015**, *3* (1), 014906.
(22) Deng, Y.; Miyake, T.; Keene, S.; Josberger, E. E.; Rolandi, M. Proton Mediated Control of Biochemical Reactions with Bioelectronic pH Modulation. *Sci. Rep.* **2016**, *6* (1), 24080.
(23) Chen, Y.; Méhes, G.; Liu, B.; Gao, L.; Cui, M.; Lin, C.; Hirono-Hara, Y.; Hara, K. Y.; Mitome, N.; Miyake, T. Proton Logic Gate Based on a Gramicidin-ATP Synthase Integrated Biotransducer. *ACS Appl. Mater. Interfaces* **2024**, *16* (6), 7480−7488.
(24) Poghossian, A.; Katz, E.; Schöning, M. J. Enzyme Logic AND-Reset and OR-Reset Gates Based on a Field-Effect Electronic Transducer Modified with Multi-Enzyme Membrane. *Chem. Commun.* **2015**, *51* (30), 6564−6567.

(25) Chen, Y.; Cui, M.; Lin, C.; Liu, B.; Mitome, N.; Miyake, T. Enzymatic Bioluminescence Modulation with an ATP Synthase Integrated Biotransducer. *Adv. Mater. Technol.* **2022**, *7*, 2100729.
(26) Bakker, E.; Bühlmann, P.; Pretsch, E. Polymer Membrane Ion-Selective Electrodes—What Are the Limits? *Electroanalysis* **1999**, *11* (13), 915—933.
(27) Si, P.; Bakker, E. Thin Layer Electrochemical Extraction of Non-Redoxactive Cations with an Anion-Exchanging Conducting Polymer Overlaid with a Selective Membrane. *Chem. Commun.* **2009**, No. 35, 5260—5262.
(28) Mitome, N.; Sato, H.; Tomiyama, T.; Shimabukuro, K.; Matsunishi, T.; Hamada, K.; Suzuki, T. Identification of Aqueous Access Residues of the Sodium Half Channel in Transmembrane Helix 5 of the F_o-*a* Subunit of Propionigenium Modestum ATP Synthase. *Biophys. Physicobiol.* **2017**, *14*, 41—47.
(29) Yue, J.; Epstein, A. J. Electronic Control of pH at Sulfonated Polyaniline Electrodes. *J. Chem. Soc., Chem. Commun.* **1992**, No. 21, 1540.
(30) Zhang, Z.; Kashiwagi, H.; Kimura, S.; Kong, S.; Ohta, Y.; Miyake, T. A Protonic Biotransducer Controlling Mitochondrial ATP Synthesis. *Sci. Rep.* **2018**, *8* (1), 10423.
(31) Cui, M.; Takahashi, M.; Chen, Y.; Liu, B.; Ohta, Y.; Miyake, T. pH Modulation in Adhesive Cells with a Protonic Biotransducer. *Bioelectrochemistry* **2022**, *147*, 108202.
(32) Crespo, G. A.; Bakker, E. Dynamic Electrochemistry with Ionophore Based Ion-Selective Membranes. *RSC Adv.* **2013**, *3* (48), 25461—25474.
(33) Bobacka, J.; Grzeszczuk, M.; Ivaska, A. Electrochemical Study of Poly(3-Octylthiophene) Film Electrodes. Impedance of the Polymer Film Semiconductor-Electrolyte Interface. *Electrochim. Acta* **1992**, *37* (10), 1759—1765.
(34) Cuartero, M.; Acres, R. G.; De Marco, R.; Bakker, E.; Crespo, G. A. Electrochemical Ion Transfer with Thin Films of Poly(3-Octylthiophene). *Anal. Chem.* **2016**, *88* (13), 6939—6946.
(35) Cuartero, M.; Crespo, G. A.; Bakker, E. Ionophore-Based Voltammetric Ion Activity Sensing with Thin Layer Membranes. *Anal. Chem.* **2016**, *88* (3), 1654—1660.
(36) Lyu, Y.; Gan, S.; Bao, Y.; Zhong, L.; Xu, J.; Wang, W.; Liu, Z.; Ma, Y.; Yang, G.; Niu, L. Solid-Contact Ion-Selective Electrodes: Response Mechanisms, Transducer Materials and Wearable Sensors. *Membranes* **2020**, *10* (6), 128.
(37) Soga, N.; Kinosita, K.; Yoshida, M.; Suzuki, T. Kinetic Equivalence of Transmembrane pH and Electrical Potential Differences in ATP Synthesis*. *J. Biol. Chem.* **2012**, *287* (12), 9633—9639.

https://doi.org/10.1021/acsami.4c05499
ACS Appl. Mater. Interfaces 2024, 16, 37521—37529